molecules

MDPI

Article

Acetylenic Fatty Acids and Stilbene Glycosides Isolated from *Santalum yasi* Collected from the Fiji Islands

Khalid AL Maqbali[1,2], Miriama Vuiyasawa[3], Mercy Ayinya Gube-Ibrahim[4,5], Shubham Sewariya[1,6], Clément Balat[1,7], Kirsti Helland[8], Tamar Garcia-sorribes[1], Mercedes de la Cruz[9], Bastien Cautain[9], Jeanette Hammer Andersen[8], Fernando Reyes[9], Jioji N. Tabudravu[1,*]

[1] School of Pharmacy and Biomedical Sciences, University of Lancashire, PR1 2HE, Preston, United Kingdom; khalid85@squ.edu.om; shubhamsewariya94@gmail.com; TGarcia-sorribes@uclan.ac.uk; clement.balat@viacesi.fr; JTabudravu@uclan.ac.uk

[2] Chemistry Department, College of Science, Sultan Qaboos University, Muscat, AL Khoudh, Sultanate of Oman; khalid85@squ.edu.om

[3] Institute of Applied Sciences, University of the South Pacific, Private Mail Bag, Suva, Fiji; miriamavuiyasawa@gmail.com

[4] Marine Biodiscovery Centre, Department of Chemistry, Meston Walk, University of Aberdeen, AB24 3UE, Scotland, United Kingdom; m.gube-ibrahim.22@abdn.ac.uk

[5] Department of Chemistry, College of Education Akwanga, Nasarawa State, Nigeria; m.gube-ibrahim.22@abdn.ac.uk

[6] Department of Chemistry, University of Delhi, New Delhi, 110007, India; shubhamsewariya94@gmail.com

[7] CESI Engineering School, Pôle Aéropolis – 1 cours de l'Industrie 64510 Assat, France; clement.balat@viacesi.fr

[8] Marbio, UiT The Arctic University of Norway, Breivika, Tromsø, Norway; kirsti.helland@uit.no; jeanette.andersen@uit.no

[9] Fundacion MEDINA, Centro de Excelencia en Investigaci on de Medicamentos Innovadores en Andalucía, Avenida del Conocimiento 34, Parque Tecnol ogico de Ciencias de la Salud, 18016, Armilla, Granada, Spain; mercedes.delacruz@medinaandalucia.es; cautainbastien@gmail.com; *mercedes.delacruz@medinaandalucia.es;* fernando.reyes@medinaandalucia.es;

* Correspondence: JNT. JTabudravu@uclan.ac.uk

Academic Editor: Firstname Lastname

Received: date
Revised: date
Accepted: date
Published: date

Citation: To be added by editorial staff during production.

Abstract

In our continuing search for new anticancer and/or antimicrobial compounds from natural products we screened for these activities in bark and leaf extracts of sandalwood plants collected from the Fiji Islands and found *Santalum yasi* to be the most active. Resulting chemical workup enabled the isolation and structural characterization of a new acetylenic acid, methyl (*E*)-octadec-6-en-8-ynoate (**1**), and an atropisomeric stilbene glycoside (**4**) (Yasibeneoside) together with six known compounds: 11,13-octadecadien-9-ynoic acid (**2**), methyl octadeca-9,11-diynoate (**3**), gaylussacin (**5**) chrysin-7-beta-monoglucoside (**6**), neoschaftoside (**7**), and chrysin-6-C-glucoside-8-C-arabinoside (**8**). Compound **1** (18:2 (6t, 8a) is an example of an Δ^6, Δ^8 acetylenic system containing the *trans* double bond at C-6 and the triple bond at C-8 which is reported here for the first time. All molecular structure elucidations and dereplications were performed using spectroscopic techniques including 2D NMR and HRMS-MS/MS spectrometry. Methyl (*E*)-octadec-6-en-8-ynoate showed moderate

activity with an IC_{50} of 91.2 ug/mL against the cancer human breast adenocarcinoma cell line MCF-7.

Keywords: *Santalum yasi*, *Santalum album*, *Santalum yasi-album* hybrid, acetylenic fatty acids Stilbene, cytotoxic

1. Introduction

Sandalwood represents a group of important medicinal and commercial plants belonging to the family Santalaceae, and the genus *Santalum*[1,2]. There are about 19 species of sandalwood known[3] of which one, *S. yasi* is endemic to Fiji[4,5] and Tonga[6]. A successful genetic hybrid between *S. yasi* and *S. album* (native to India)[7] is also growing in Fiji[8]. *Santalum yasi* like other sandalwood is a hemi-parasitic plant with a very slow growth rate (about 0.3-0.7 m per year) with mature trees reaching heights of about 10 metres[4]. *S. yasi* has traditionally been used in Fiji for medicine, incense, and in wedding ceremonies[9]. Commercially, *S. yasi* has often been regarded to be of high value due to its high content in α-, and β-santalols that typically meets the East Indian Sandalwood ISO standard for sandalwood oil[5]. Most chemical investigative studies have been carried out on essential oil content of sandalwood[10–14], but studies on other compounds[14] in sandalwood such as *S. yasi* is lacking. To date no literature exists on the phytochemical content of leaves or bark of *S. yasi* making this study the first of its kind to shed light on the phytochemistry of *S. yasi*. While screening for cytotoxicity and antimicrobial activities in sandalwood plants from Fiji, significant activities were observed in the bark fractions of *S. yasi*, and the *S. yasi-album* hybrid species against methicillin-sensitive *Staphylococcus aureus* (MSSA ATCC-29213), and *Candida albicans* (*C. albicans* ATTCC-64124), and the cancer cell lines A549 (human lung carcinoma), A2058 (human Caucasian metastatic melanoma), HepG2 (human liver carcinoma cells), MCF-7 (human breast adenocarcinoma), MIA Paca-2 (human Caucasian pancreatic carcinoma), and PC-3 (human Caucasian prostate adenocarcinoma). Cytotoxicity activities were also observed in *S. album* leaf fractions against the cancer cell lines A2058, HepG2, and MCF-7. The report describes biological activities of fractions of the three sandalwood species in Fiji and the structure elucidation of compounds isolated from *S. yasi*.

2. Results and Discussion

Bark and leaves of the three sandalwood plants were collected in Fiji and extracted with methanol (MeOH) followed by dichloromethane (DCM) to produce six crude extracts. Each crude extract was then processed using a modified Kupchan[15] liquid-liquid partitioning method to produce four fractions based on polarity: water-butanol (WB), water-methanol (FM), dichloromethane (FD), and hexane (FH) (Figure S72). All fractions were screened for bioactivity against five clinically important human microbial pathogens (Table S70), and against six cancer cell lines (Table S71) with both *S. yasi* and the *S. yasi-album* hybrid bark fractions showing the most promising results (Figure 4). The *S. yasi* bark hexane fraction (SyB-FH) that had displayed good activity against MSSA and against four of the cancer cell lines was purified further on a Sephadex LH-20[16] column using MeOH-DCM (1:1) followed by reversed phase purification on a C_{18} HPLC column using a H_2O-CH_3CN (40-60) solvent isocratic system to afford the new compound methyl (*E*)-octadec-6-en-8-ynoate (**1**), and the known compounds 11,13-octadecadien-9-ynoic acid (**2**), methyl octadeca-9,11-diynoate (**3**).

The dichloromethane fraction of *S. yasi* leaf (SyL-FD) was fractionated on a C_{18} solid phase extraction column (SPE) using 50% H_2O-MeOH and further purified on a C_{18} HPLC column using H_2O-MeOH gradient system to afford 2.8 mg of yasibeneoside **(4)**, and the known compounds gaylussacin (**5**) chrysin-7-beta-monoglucoside (**6**), neoschaftoside (**7**), and chrysin-6-C-glucoside-8-C-arabinoside (**8**).

2.1 Structure Elucidation

Compound **1** showed a HRESIMS ion at *m/z* 293.2475 $[M + H]^+$ (Δ 1.0 ppm) (Figure S11) for the expected molecular formula of $C_{19}H_{32}O_2$ with 4 indices of hydrogen deficiency[17,18]. Interpretation of ^{13}C, HSQC, and HMBC NMR data (Figures S1-10), Table 1) of **1** showed the presence of 19 carbons in the

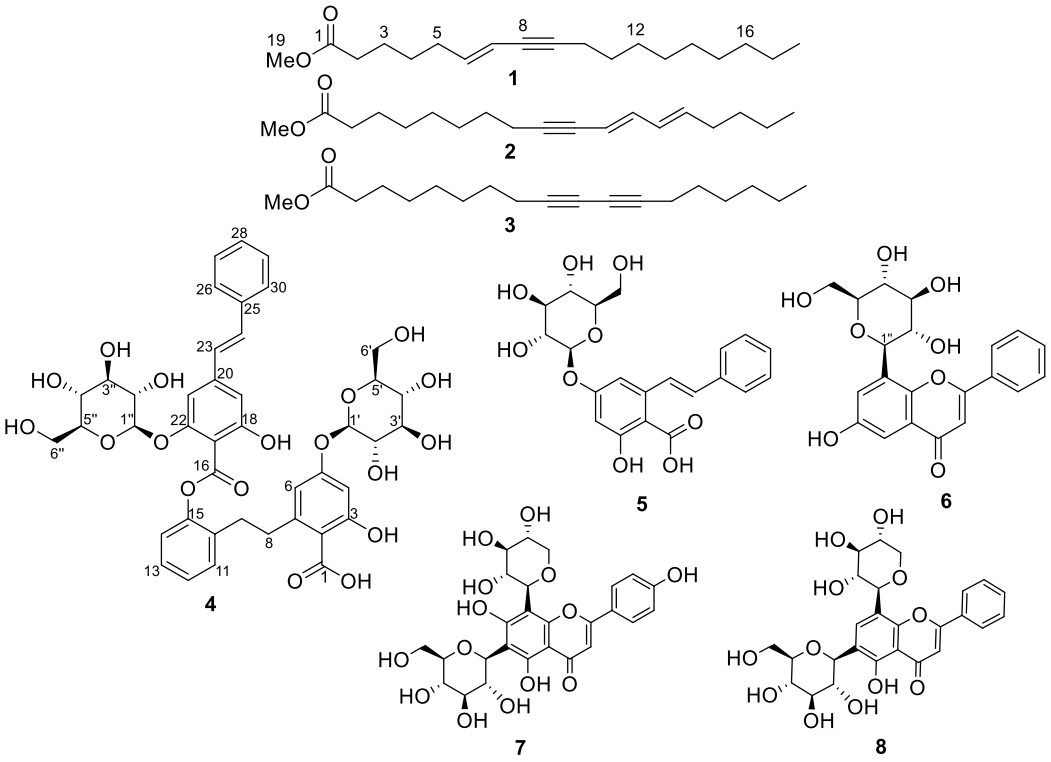

.

form of 2 methyl groups (δ_C, 50.7, 13.0), 12 sp^3 methylenes (δ_C 33.4, 32.5, 31.4, 28.7, 28.6, 28.5, 28.4, 28.3, 26.1, 24.6, 22.3, 18.5), 2 sp^2 methines (δ_C 142.5, 109.8), 2 non-protonated sp carbons (δ_C 87.7, 78.9), and one ester carbonyl (δ_C 174.8). Two sp^2 plus two sp carbons, plus one ester carbonyl accounted for the 4 indices of deficiency indicating the structure of **1** was linear. Interpretation of 1D and 2D NMR (Figures S1-10) data enabled the construction of two substructures (Figure 1). The position of the ester group was established by HMBC correlations of the methoxy proton at δ_H 3.60 (H-19), and methylenes at δ_H 2.27 (H-2), 1.56 (H-3) to the ester carbon at δ_C 174.8 (Table 1). Key COSY correlations between the methine proton at δ_H 5.92 (H-6), and δ_H 5.38 (H-7) to the methylene proton δ_H 2.02 (H-5) (Figure S4-5), HMBC correlations between the methine proton δ_H 5.92 (H-6) to the carbon at δ_C 32.5 (C-5) and the methylene protons at δ_H 2.27 (H-2), 1.56 (H-3), 2.02 (H-5) to the carbon at δ_C 28.6 (C-4) (Figures S7-9) unambiguously established the position of the alkene unsaturation at C-6/C-7. HMBC correlations between δ_H 5.38 (H-7) to the carbon at δ_C 87.7 (C-9) and between δ_H 5.92 (H-6) to δ_C 87.7 (C-8) (Figure S10, Table 1) established the 'ene-yne' spin system. The *E* geometry of the double bond in the molecule was secured through a ^{1}H-^{1}H coupling constant of 15.7 Hz between H-6 and H-7. Further evidence for the proposed structure came from NMR chemical shift predictions. A plot of ^{13}C experimental data against predicted data calculated by ACD/Labs Structure Elucidator[19] using the HOSE[20] code is shown in Figure 2 with a linear regression of r^2 = 0.9997 suggesting that the proposed structure is most likely correct[21,22]. This strategy has been shown to be effective in predicting correct structures of natural products[22,23]. Additional evidence for the structure of **1** was provided by HR-MS/MS

fragmentation data which has been annotated with fragments calculated by the ACD/labs MS Fragmenter[24] software (Figure S12). The presence of compound **1** as a methyl ester rather than an acid can be evidenced by the presence of proton NMR signals between δ_H3-6-3-9 ppm on the semi-crude extract (^{1}H NMR not shown). In addition, the solvent system used for the extraction of **1** from the bark of *S. yasi* was also used to extract the seed oil of *S. album*. ^{1}H NMR of the seed oil of *S. album* showed the presence of ximenynic acid (Figure S74) and not its methyl ester. Both data suggest that compound **1** is a natural product rather than an artifact of extraction and purification.

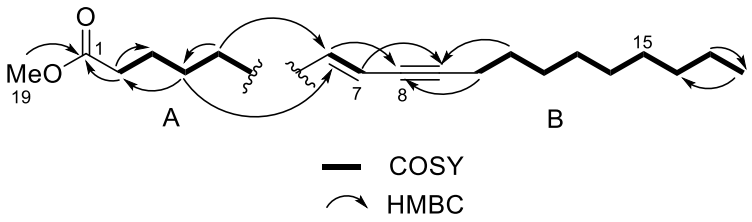

Figure 1. Substructures A and B showing key COSY and HMBC correlations establishing positions of unsaturation in the structure of **1**.

Table 1. NMR Spectroscopic Data (600/150 MHz, CD_3OD) for Compound 1

Pos.	δ_C, type	δ_H (*J* in Hz)	COSY ^{1}H–^{1}H	HMBC ^{1}H→^{13}C
1	174.8, C			
2	33.4, CH_2	2.27, t, 7.6	3	1, 3, 4
3	24.6, CH_2	1.56, t, 7.4	2, 4	1, 2, 4, 6
4	28.6, CH_2	1.28, ovlp[a]	3,4	6
5	32.5, CH_2	2.02, m	4, 6, 7	6, 5
6	142.5, CH	5.92, m	4,7	8
7	109.8, CH	5.38, d, 15.7	5, 6, 5	9
8	78.9, C			

9	87.7, C			
10	18.5, CH_2	2.20, t, 7.5	11	8, 9
11	28.5, CH_2	1.45, ovlp	10	9
12	28.4, CH_2	1.36, ovlp	11, 13	10
13	28.3, CH_2	1.32, ovlp	12, 14	
14	28.2, CH_2	1.28, ovlp	13,15	
15	28.1, CH_2	1.29, ovlp	14,16	
16	31.4, CH_2	1.24, ovlp	15, 17	15, 17
17	22.3, CH_2	1.26, ovlp	16,17	18
18	13.0, CH_3	0.85, t, 7.02	17, 19	16, 17, 31
19	50.7, CH_3	3.60, s	18	1

[a]Ovlp = overlap

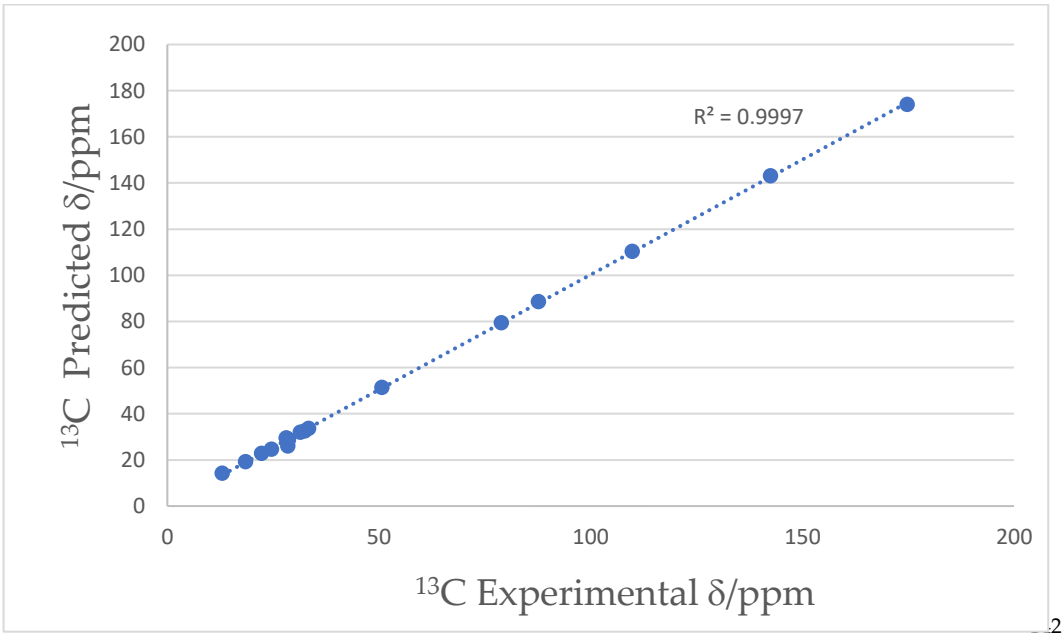

Figure 2. Plot of ^{13}C experimental vs predicted chemical shifts data for **1**.

Compound **4** showed a HRESIMS ion at *m/z* 837.2587 $[M+H]^+$ calculated for $C_{42}H_{45}O_{18}$ (837.2606, Δ = 1.6 ppm) with 21 indices of hydrogen deficiency (Figure S27). Interpretation of Edited-HSQC, and HMBC NMR data (Figures S17-18, Table 2) indicated the presence of 42 carbons including 15 sp^2 methines (δ_C 130.8, 129.0, 129.0, 128.9, 128.1, 127.4, 127.3, 126.3, 126.3, 125.4, 125.4, 111.0, 107.4, 102.9, 101.8), 10 sp^3 methines (δ_C 100.1, 99.9, 77.0, 76.9, 76.8, 76.5, 73.4, 69.9, 69.8), 4 sp^3 methylenes (δ_C 61.1, 61.0, 38.5, 37.9) and 13 sp^2 quaternary carbons (δ_C 172.9, 172.7, 164.7, 164.0, 161.6, 161.5, 151.5, 147.1, 142.8, 142.0, 137.6, 106.4, 106.2). The 4 benzene ring systems plus one alkene plus one ester linkage plus one carboxylic acid group fully accounted for the 21 indices of hydrogen deficiency in the structure of **4**. Extensive interpretation of one- and two-dimensional NMR data (Figures S15-18) enabled the construction of 6 substructures (Figure 3).

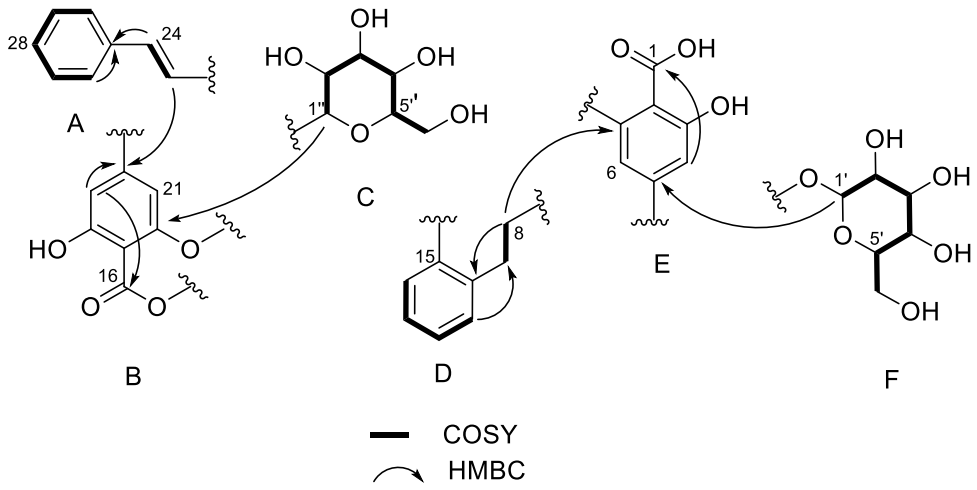

Figure 3. Substructures A-F derived from COSY (bold line) and HMBC correlations (H to C, blue arrows) for **4.**

The six substructures or spin systems include: one mono-substituted benzene ring coupled to an alkene system (substructure A), two 1,2,3,5-tetra-substituted benzene rings (substructures B and E), one 1,2-di-substitued benzene ring linked to an ethyl moiety (substructure D), and two glycosidic spin systems (substructures C and F). Long range HMBC correlations were used to connect these substructures to attain the full structure of **4**. HMBC correlations were observed between the proton signal at δ_H 6.91 (H-23) to the sp^2 carbon at δ_C 142.8 (C-20) linking substructures A to B. Similarly, HMBC correlations were observed between the diastereotopic protons at δ_H 3.20/3.17 (H-8) to the sp^2 quaternary carbon at δ_C 147.1 (C-7) linking substructures D and E. Despite the absence of HMBC correlations between substructures B and D, substructure B was most likely linked to substructure D at C-15 based on the chemical shift of this carbon (δ_C 151.5) suggesting that C-15 was linked to C-16 via an ester linkage. A HMBC correlation between the anomeric proton at δ_H 5.05 (H-1'') and the sp^2 quaternary carbon at 161.6 ppm (C-22) linked one of the glycosides

(substructure C) to substructure B. The second glycoside (substructure F) was linked to substructure E through an observed HMBC correlation between the anomeric proton at δ_H 4.89 (H-1′) to the sp² quaternary carbon at δ_C 161.5 (C-5) to complete the planar structure for **4**. Additional proof for the structure of **4** was obtained by plotting predicted and experimental ^{13}C NMR data (Figure S26). A strong correlation ($R^2 = 0.9996$) was obtained suggesting that the proposed planar structure for **4** is most likely correct[21,25]. Further evidence for the structure for **4** was provided by analysis of HRMS/MS fragmentation data (Figure S28).

The geometry of the alkene system at C-23/C-24 was determined to be *E* based on the large coupling constant of 16.0 Hz between H-23 and H-24. The relative configurations of the two glycoside units were determined to be β based on coupling constant of 7.4 Hz between H-1′ and H-2′, and 6.9 Hz for H-1′′ and H-2.′′. Further evidence was shown by NOE correlations between H-1′ and H-3′/H-4′; H-2′′ and H-3′′/H-4′′(Table 2, Figures S19-22). NMR data show that the protons of the CH_2 group at C-8, as well as C-9 resonate at different chemical shifts (Figures S15-19) suggesting chirality associated with atropisomers [26,27]. The tentative room temperature conformation of the structure of **4** is supported by key NOE correlations between H-8A/B and H-9A/B to H-11 and H-6 (Figures S19, S23-24). Figure S25 shows the minimized energy structure calculated using Chem3D Ultra[28]. The structure shows key H-bonding between the carbonyl group C-1 (carboxylic acid), and the hydroxy group at C-4′′, hindering free rotation between C-8 and C-9 resulting in chemical and magnetic non-equivalence of the methylene protons at C-8/C-9[29–31]. Due to sample limitation optical rotation and circular dichroism (CD) spectra were not measured for compound **4**.

Table 2. NMR Spectroscopic Data (800/200 MHz, CD_3OD) for Compound 4

Pos	δ_C, [a]type	δ_H (J/Hz)	COSY ^1H–^1H	HMBC $^1H \rightarrow ^{13}C$	NOESY
1	172.9, C				
2	106.4, C				
3	164.7, C				
4	101.8, CH	6.50, d, 7.4		1, 3, 5	
5	161.5, C				
6	111.0, CH	6.46, d, 2.3		1, 5, 7	8A, 8B
7	147.1, C				
8	38.5, CH_2	A: 3.20, m	9	2, 6, 7, 10	6, 11
		B: 3.17, m	9	2, 7,10	6, 11
9	37.9, CH_2	A: 2.89, m	8A, 8B	7, 10	6, 11
		B: 2.85, m	8A, 8B	7, 10	6, 11
10	142.0, C				
11	128.2, CH	7.22, d, 8.0	12	10, 12, 15	8A, 8B, 9A, 9B
12	125.6, CH	7.17, t, 7.7	11	13	
13	128.0, CH	7.26, t, 8.0	14	12, 15	

14	127.6, CH	7.17, d, 8.0	13	12, 15	
15	151.5, C				
16	172.7, C				
17	106.2, C				
18	164.0 C				
19	102.9, CH	6.60, d, 2.3	21	16, 17, 18, 21, 23	
20	142.8, C				
21	107.4, CH	6.92, d, 2.2	19	16, 17, 19, 22, 23	
22	161.6, C				
23	128.9, CH	6.91, d, 16.0	24	19, 20	
24	130.8, CH	7.98, d, 16.0	23	20, 24	
25	137.6, C				
26	126.3, CH	7.52, d, 8.0	28	25, 27, 28	
27	129.0, CH	6.95, d, 8.0	28, 26	25, 28	
28	128.0, CH	7.35, d, 8.0	27, 26		
29	129.0, CH	6.95, d, 8.0	28, 30	25, 28	
30	126.3, CH	7.52, d, 8.0	28, 29	25, 27, 28	
1'	99.9, CH	4.74, d, 7.0	2'	2', 5	3' 4'
2'	73.4 CH	3.49, m	1', 3'		
3'	76.8, CH	3.39, m	2', 4'	2'	1'
4'	69.8, CH	3.48, m	3'		1'
5'	76.5, CH	3.44, m	4'	5'	
6'	61.0, CH_2	A: 3.91, dd, 11.8, 2.2	5'		
		B: 3.72, m	5'		
1''	100.1, CH	5.05, d, 7.0	2''	22	3'', 4''
2''	73.4, CH	3.50, m	1'', 4''	2''	
3''	76.9, CH	3.46, m	2'', 4''		1''
4''	69.9, CH	3.41, m	3''	2''	1''
5''	77.0, CH	3.53, m	4'', 6''A, 6''B		
6''	61.1, CH_2	A: 3.93, dd, 11.8, 2.2	5''	5''	
		B: 3.72, m	5''		

[a]Carbons extracted from 2D NMR (HSQC and HMBC)

Compound **2** showed an *m/z* of 291.2318 $[M+H]^+$ calculated for $C_{19}H_{31}O_2$ (291.2319, Δ = -0.2 ppm) (Figure S40). Interpretation of ^1H, 2D NMR and HR-MS/MS data (Figures S31-39, S41-42) identified **2** as 11,13-octadecadien-9-ynoic acid[32].

Compound **3** showed an *m/z* of 291.2319 $[M+H]^+$ calculated for $C_{19}H_{31}O_2$ (291.2319, Δ = 0.4 ppm) (Figure S48). Interpretation of ^1H, 2D NMR and HR-MS/MS data (Figures S43-47, S49) identified compound **3** as methyl octadeca-9,11-diynoate[33].

Compound **5** showed an *m/z* of 419.1347 M+H]$^+$ calculated for $C_{21}H_{23}O_9$ (419.1342, Δ = -2.5 ppm) (Figure S54). Interpretation of ^{1}H, and 2D NMR data (Figures S50-53) identified compound **5** as gaylussacin[33,34].

Compound **6** showed an *m/z* of 417.1191 M+H]$^+$ calculated for $C_{21}H_{21}O_9$ (417.1186, Δ = -2.6 ppm) (Figure S59). Interpretation of ^{1}H, ^{13}C and 2D NMR data (Figures S55-58) identified the compound as chrysin-7-beta-monoglucoside[35,36].

Compound **7** showed an *m/z* of 565.1570 M+H]$^+$ calculated for $C_{26}H_{29}O_{14}$ (565.1557, Δ = 2.9 ppm) (Figure S64). Interpretation of ^{1}H, and 2D NMR data (Figures S60-63) identified the compound as neoschaftoside[37,38].

Compound **8** showed an *m/z* of 549.1618 M+H]$^+$ calculated for $C_{26}H_{29}O_{13}$ (549.1608, Δ = 2.9 ppm) (Figure S69). Interpretation of ^{1}H, and 2D NMR data (Figures S65-68) identified the compounds as chrysin-6-C-glucoside-8-C-arabinoside[39].

2.2 *Biological Activity*

The modified Kupchan fractions of leaf and bark of *S. yasi*, *S. album*, and *S. yasi-album* hybrid were screened for antibacterial, antifungal, and cytotoxic activities. Leaf fractions of the three sandalwood plants displayed low to mild activity at 0.32 mg/mL against the pathogens tested (Table S70) with the butanol (WB) fraction of the bark of *S. yasi* showed good activity against *Candida albicans*. The strongest activities were shown by the FH fractions of the bark of *S. yasi*, and *S. yasi-album* hybrid against MSSA ATCC-29213 (>90% inhibition) (Figure 4b, Table S70).

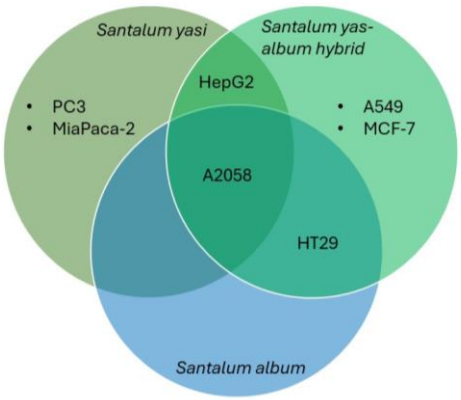

4a

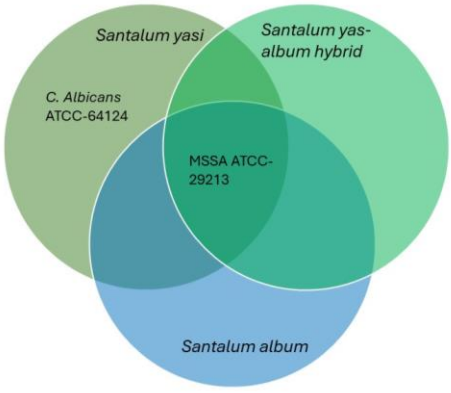

4b

Figure 4a. Cytotoxic activity of the bark hexane fractions of *S. yasi*, *S. album*, and *S. yasi-album* hybrid. A549 (human lung carcinoma), A2058 (human Caucasian metastatic melanoma), HepG2 (human liver carcinoma cells), MCF7 (human breast adenocarcinoma), MiaPaca-2 (human Caucasian pancreatic carcinoma), and PC-3 (human Caucasian prostate adenocarcinoma), HT-29 (human colorectal adenocarcinoma). Both *S. yasi* and *S. yasi-album* hybrid were active at 0.10 mg/mL while *S. album* was active at 0.05 mg/mL (Table S71). 4b. Antimicrobial assay activity. MSSA ATCC-29213 (Methicillin-susceptible *Staphyloccocus aureus* subspecies *aureus* strain Wichita), *C. albicans* ATCC-64124 (*Candida albicans*). The *C. albicans* activity (>50% inhibition, Table S70) was reported only in the WB fraction while the MSSA activity

were recorded in the bark FH fractions of the three sandalwood plants. Antimicrobial assays of fractions were performed at 0.06 mg/mL.

For the cytotoxicity assay both *S. yasi bark* (FH), and *S. album* leaf (FM) showed activity (60-90%) at 0.10 mg/mL against human Caucasian metastatic melanoma (A2058), human liver carcinoma cells (HepG2), human breast(adenocarcinoma) (MCF7), human Caucasian pancreatic carcinoma (MIA PaCa-2), and human Caucasian prostate adenocarcinoma (PC-3) with the strongest activity shown by the *S. yasi* bark fraction (FH) at 90% inhibition of HepG2 cells. *S. yasi-album* hybrid bark (FH) inhibited both human lung carcinoma (A549) and human colorectal adenocarcinoma (HT-29) in addition to the cell lines inhibited by *S. yasi and S. album* (Figure 4a, Table S71).

Methyl (*E*)-octadec-6-en-8-ynoate (**1**) showed an IC_{50} of 91.2 ug/mL (Figure S73) but showed no activity against A2058 and human fibroblast cells (MRC-5). Compounds **5**-**8** showed weak cytotoxic activity (results not shown).

3. Materials and Methods

3.1. Reagents and Solvents

All solvents used for chromatography purifications were HPLC grade, while LCMS solvents were MS grade, both were obtained from Fisher Scientific[40], and NMR solvents were obtained from Goss Scientific[41].

3.2 Main Instruments

UV spectra were recorded on an Agilent Technologies 1220 Infinity Photodiode array detector[42]. IR spectra were recorded on a Shimadzu fourier transform infrared spectrophotometer (IRTracer-100)[43]. NMR spectroscopic data for compounds **4-8** were recorded at the University of Edinburgh[44] at 25 °C on a Bruker Avance NEO 800 MHz with a He-cooled cryoprobe Compounds **1-3** were recorded at the Biodiscovery Centre, University of Aberdeen[45] on a Bruker AVANCE III HD Prodigy TCI cryoprobe at 600 and 150 MHz for ^{1}H and ^{13}C, respectively. This instrument was optimized for ^{1}H observation with pulsing/decoupling of ^{13}C and ^{15}N with ^{2}H lock channels equipped with shielded z-gradients and cooled preamplifiers for ^{1}H and ^{13}C. The ^{1}H and ^{13}C chemical shifts were referenced to the solvent signals (δ_H 3.31 and δ_C 49.00 in CD_3OD). LC-HRESIMS analysis for compounds **1-4** were performed on an Agilent 1290 LC system with a photodiode array detector (DAD) coupled to an Agilent 6546 LC-QTOF equipped with dual spray jet stream technology electrospray ion source (AJS)[42]. The system was controlled by the Mass Hunter 11.0[46] software. Liquid chromatographic separations were performed at 40 °C on a Kinetex phenyl hexyl 100 × 3.0 mm, 1.7 μm (Phenomenex)[47] equipped with a security guard column. A linear CH_3CN-H_2O gradient of 20% CH_3CN−water to 100% CH_3CN in 12 min was applied at a constant flow of 0.4 mL/min; then 100% CH_3CN was maintained for a 3 min before returning to the starting conditions in 1 min and equilibrating for a further 3 min. Formic acid (0.1% v/v) was added to all solvents and UV spectra were collected by a DAD from 200 to 500 nm with a resolution of 2 nm. Tuning in ESI^+ mode was performed using Agilent's tuning mix[42] of 6 masses to a resolution of FWHM between 40,495 for $[M+H]^+$ of

118.086255 at the lower end and 64,549 for 1521.971475 at the upper end giving rise to an average accuracy of <1.0 ppm within the mass range. Mass accuracy was maintained throughout sample analysis via use of dual spray technology using Agilent's reference solution mix[42]. Scanning source parameters for ESI^+ were as follows: capillary (3,500 V), nozzle (1,000 V), fragmentor (190 V), skimmer1 (65 V), and octapole RF peak (750 V). Targeted MS^2 (ES^+) fragmentation mode for compound **1** (*m*/*z* 293.2501) was performed at four collision energies: 10, 20, 30, 40 V at peak retention time (t_R) of 9.80 +/- 0.06 min. Targeted MS^2 (ES^-) fragmentation mode for compound **4** (*m*/*z* 835.2455) was performed at four collision energies: 5, 10, 15, 30 V at peak retention time (t_R) of 3.08 +/- 0.06 min.

LC-HRESIMS for compounds **5-8** were performed on a Bruker Maxis II Time of Flight instrument[45,48] using the following parameters: capillary voltage 45 V, capillary temperature 320 °C, auxiliary gas flow rate 10−20 arbitrary units, sheath gas flowrate 40−50 arbitrary units, spray voltage 4.5 kV, mass range 100−2000 amu, resolution 80 000 for HRESIMS.

3.3 Chomatography

Sephadex LH-20[49] was sourced from Merk[16]. Solid phase extractions were performed using Phenomenex C18 cartridges (Strata C18-E, 55 um, 70 Å)[50]. Semipreparative HPLC purifications were performed on an Agilent 75 1100 HPLC system consisting of a binary pump, degasser, photodiode array detector.

3.4 Plant Collection and Extraction

Sandalwood leaves and bark were collected from the Fiji Islands: *S. yasi* from 114 Milverton road, Suva (-18.1349, 178.4476)[51], *S. album* from Vavalagi road, Nakasi (-18.06517, 178.5154)[51,] and *S. yasi-album* hybrid from Yauvula, Wainunu, Bua (-16.805842, 178.889114)[51]. All samples were taken to the Institute of Applied Sciences, University of the South Pacific[52], Suva for processing. All plants were taxonomically identified based on morphological features at the South Pacific Regional Herbarium[53] where voucher specimens are kept with the following collection numbers: *S. yasi* (Tuiwawa5237), *S. album* (Tuiwawa5238), and *S. yasi-album* hybrid (Tuiwawa5239). Bark (10 g) and leaves (5 g) were extracted separately with methanol (3×) followed by dichlomethane (DCM 3×). Extracts were dried under vacuum, and fractionated using the modified Kupchan liquid-liquid partitioning technique[15,54](Figure S72) to produce four fractions: hexane (FH), dichloromethane (FD), methanol-water (FM) and butanol-water (WB). The process is summarized as follows: The crude sample was dissolved in water (30 mL) and partitioned with DCM (30 mL). The aqueous layer was then partitioned with secondary butanol (30 mL) to produce the WB fraction. The DCM fraction was dried under rotary evaporation, dissolved in 90% methanol-water (30 mL), and partitioned with n-hexane (30 mL) to yield the FH fraction. The 90% methanol-water layer was phase adjusted to 50% methanol-water and partitioned with DCM (54 mL) to yield the FM and FD fractions respectively. Each of the steps described above was repeated three times to enhance separation efficiencies. These four fractions (WB, FM, FD, and FH) were dried and shipped to the University of Lancashire in the United Kingdom.

3.5 Purification and Isolation

The FH fraction of the bark of *S. yasi* was subjected to size exclusion chromatography using the Sephadex LH-20 gel as stationary phase eluted with dichloromethane-MeOH (1:1) to yield 10 Sephadex fractions. The most interesting fraction in terms of ^{1}H NMR profile was fraction Sephadex-4 (S-4) which was subjected to HPLC purification on a Waters Sunfire C18 OBD™ semi-Prep column (250×10 mm) using a solvent gradient from 0 to 100% CH_3CN in 25 min and maintained at 100% CH_3CN for a further 10 min with a flow rate of 1.5 mL/min to yield 2.5 mg (0.025% ww) of **1**, 2.3 mg (0.023% ww) of **2**, and 1.8 mg (0.018% ww) of **3**.

The FD fraction of the leaf extract of *S. yasi* was fractionated further into four sub-fractions using reversed phase C-18 SPE cartridges where after conditioning of the column as recommended by Phenomenex[50], the column was flushed with 100% water to remove salts and other polar compounds followed by 25%, 50% and 100% (MeOH-H_2O). After drying under nitrogen flow, fractions were profiled by ^{1}H NMR with the SPE-50% fraction selected for further purification on an ACE 5 C18 HL 250 × 10 mm using an isocratic solvent system of 30% CH_3CN-H_2O at a flow rate of 1.5 mL/min to yield 3.0 mg (0.060% ww)of **4**, 1.9 mg (0.038% ww) of **5**, 1.8 mg (0.036% ww) of **6.**

3.6 Cytotoxicity Assays

Cytotoxicity assays for compound **1** were performed as follows following the method described by Schlüter et. al.[55]: Human melanoma cells (A2058, ATCC no: CRL-1147) were grown and assayed in Dulbeccos Modified Eagles Medium (DMEM, Sigma D6171) supplemented with fetal bovine serum (FBS), glutamine stable and gentamycin. Human breast adenocarcinoma (MCF7, ATCC no HTB-22) and human lung fibroblasts, normal (MRC-5, ATCC no: CCL-171) were grown and assayed in minimum essential medium eagle (MEM, Sigma M7278) supplemented with FBS, glutamine stable, non-essential amino Acids, sodium pyruvate and gentamycin. Cells were seeded in 96-well microtiter plates and incubated for 24 hours at 37°C and 5 % CO_2. After 24 hours the samples were added at a concentration of 100 µg/mL, and the cells were incubated for 72 hours at 37°C and 5 % CO_2. Cell seeding density were 2000 cells/well for A2058 and MCF7 respectively. MR-C5 cells were seeded at 4000 cells/well. Cytotoxicity assay for **1** were measured by adding CellTiter 96 Aqueous One Solution (Promega). Metabolically active cells will reduce the yellow MTS salt to purple formazan. After 60 minutes of incubation with Aqueous One Solution, absorbance was read at 490 nm. The quantity of formazan measured at 490 nm is directly proportional to the number of living cells. Cell survival is then calculated by comparing the samples with a negative control (100 % cell survival) and a positive control (100 % cell death).

The cytotoxic activity of sandalwood fractions were tested against seven different human cancer cell lines: A549 (lung carcinoma), A2058 (metastatic melanoma), MCF7 (breast adenocarcinoma), HT-29 (colorectal adenocarcinoma MIA PaCa-2 (pancreatic carcinoma), PC-3 (prostate adenocarcinoma), and HepG2 (hepatocyte carcinoma) based on the MTT (3-(4,5-dimethylthiazol-2-yl)-2,5-diphenyltetrazolium bromide) assay[56]. Fractions were tested in duplicate following an established methodology[57].

3.7 Antimicrobial Assays

Antimicrobial testing against human pathogenic Gram Positive (methicillin sensitive *Staphylococcus aureus* (MSSA) ATCC29213 and methicillin resistant *Staphylococcus aureus* (MRSA) MB5393) and Gram Negative bacteria (*Escherichia coli* ATCC 25922, *Klebsiella pneumoniae* ATCC700603, *Pseudomonas aeruginosa* PAO-1 and *Acinetobacter baumannii* MB5973), yeast (*Candida albicans* ATCC64124) and fungi (*Aspergillus fumigatus* ATCC46645) were performed following established procedures[58]. Fractions were tested in duplicate.

4. Conclusions

The study has shown the potential of sandalwood plants as source of cytotoxic compounds in particular *S. yasi* (and *S. yasi-album* hybrid) resulting in the isolation and characterization of two new compounds, one of which compound **1**, an acetylenic acid, showing moderate cytotoxic activity against breast cancer cells, MCF-7. Even though acetylenic acids (**1-3**) have been isolated for the first time from the bark of *S. yasi*, this class of compound has been previously identified in sandalwood. Ximenynic acid has been known to occur in seeds of *S. album, S. insulare*, and others[13,59] and the compound is known for its various biological activities including anti-inflammatory, anticancer, larvicidal, and antimicrobial, and widely used in the cosmetic industries[60,61]. Unsaturated fatty acid with double and/or triple bonds have been of interest due to its potency against fungal pathogens[62] with undecylenic acid (UDA) is an example of such compound is on the market as an antifungal agent[63]. However, the position of the double and triple bond can vary[64] and bioactivity is dependent on the length of the fatty acid chain and position of unsaturation[63]. Known acetylenic acids previously isolated from *Santalum* sp. have the usual Δ^9, Δ^{12} unsaturation carbons[64]. Compound **1** has the *trans* double bond at C-6 and a triple bond at C-8 which is different from those previously reported in literature where C-6 is either a *cis*-double bond conjugated to *cis* double bonds at C-9[65] or a triple bond at C-6 either alone or in conjugation with *cis*/*trans* double[65,66] or triple bonds[63]. The closest related compounds are 6-octadecen-9-ynoic acid isolated from the nuts of *Ongokea klaineana*[67] which has a *trans* double bond at C-6, and a triple bond at C-9, and 9-octadecen-6-ynoic acid isolated from *Riccia fluitans*[66] where the *trans* double bond is at C-9, and the triple bond at C-6, hence, compound **1** is the first example of an unusual C-6/C-8 unsaturations. Furthermore, alkyne bond containing natural products such as polyacetylenes have been known for their strong antimicrobial activities[68,69] against drug resistant strains such as MRSA,[70,71] and anticancer activities[72] making them potential drug lead templates. Yasibeneoside (**4**) is the first example of a stilbene in the family Santalaceae (40 genera)[73] as stilbenes have been known only to occur in other plant families such as Vitaceae, Leguminaceae, Gnetaceae, and Dipterocaraceae[74] indicating the wide occurrence of the enzyme stilbene synthase (STS)[75] in other plant families. It adds a new structure to the stilbene family of structures that have been extensively studied for their cancer preventative, and tumour suppression effects[76–80]. Stilbene containing scaffolds such as tamoxifen and raloxifene are synthetic approved FDA drugs in clinical and have been known to lower risk for breast cancer[81] underpinning the importance of this scaffold in drug discovery and development. In addition, yasibeneoside displays atropisomerism, a property that is attracting a lot of interest in the drug discovery and drug

development field due to potential effects of various conformations on receptor binding in biological systems[27,82]. However, due to sample limitation in this study, bioactivity investigation for yasibeneoside was not carried out.

.

Supplementary Materials: The following supporting information can be downloaded at: **10.5281/zenodo.171654.**

Author Contributions: Conceptualization, J.T., M.V. K.M., M.A.G.; Methodology and Investigation, M.V., K.M., M.A.G., C.B., K.H, S.S., T.G., B.C., M.C.; data curation, S.S., T.G., B.C., M.C.; data analysis, J.T., M.A.G., T.G., S.S., K.M., K.H., M.V., C.B., J.H.A., F.R., Original draft preparation, K.M., M.V., M.G., S.S., C.B, K.H., T.G., M.C., B.C., J.H.A, F.R., J.T.; editing, review, K.M., M.V., M.G., S.S., C.B, K.H., T.G., M.C., B.C., J.H.A, F.R., J.T Supervision, J.T.; Project administration and funding, J.T. All authors have read and agreed to the published version of the manuscript.

Funding: Supported by the Tertiary Education Trust fund (TetFund) Nigeria for the MSc scholarship for M.A.G. to the University of Central Lancashire, United Kingdom; The Omani government for the MSc scholarship for K.M. to the University of Central Lancashire, United Kingdom.

Data Availability Statement: Data are contained within the article and supplementary Materials.

Acknowledgments: JT wishes to acknowledge Mr Russel Gray of the NMR facilities at the Marine Biodiscovery Centre, University of Aberdeen; Mr Juraj Bella of the NMR facilities at the University of Edinburgh; ACD/Labs for software support and providing the Structure Elucidator/MS Workbook Suite; the late Mr Iliesa Taukenatabua of 114 Milverton road, Suva, Fiji Islands for donating the *S. yasi* plant; Mr Usaia Tabudravu for donating the *S. yasi-album* hybrid plant; Mr Marika Tuiwawa of the South Pacific Herbarium, University of the South Pacific (USP, Suva, Fiji for taxonomic identification of the plants; My Joape Ginigini for use of facilities for samples extractions at the Institute of Applied Sciences, USP; Kathryn Dickens and Sameera Mahroof of the Analytical Suite, JB Firth Building, University of Lancashire for LCMS and technical support.

Conflicts of Interest: The authors declare no conflicts of interest

References

1. Diaz-Chavez, M.L.; Moniodis, J.; Madilao, L.L.; Jancsik, S.; Keeling, C.I.; Barbour, E.L.; Ghisalberti, E.L.; Plummer, J.A.; Jones, C.G.; Bohlmann, J. Biosynthesis of Sandalwood Oil: Santalum Album CYP76F Cytochromes P450 Produce Santalols and Bergamotol. *PLOS ONE* **2013**, *8*, e75053, doi:10.1371/journal.pone.0075053.

2. Boruah, T.; Parashar, P.; Ujir, C.; Dey, S.Kr.; Nayik, G.A.; Ansari, M.J.; Nejad, A.S.M. Chapter 6 - Sandalwood Essential Oil. In *Essential Oils*; Nayik, G.A., Ansari, M.J., Eds.; Academic Press, 2023; pp. 121–145 ISBN 978-0-323-91740-7.

3. Santalum L. | Plants of the World Online | Kew Science Available online: http://powo.science.kew.org/taxon/urn:lsid:ipni.org:names:30113685-2 (accessed on 31 March 2025).
4. Plants of the Fiji Islands by Parham, J.w. Available online: https://www.pemberleybooks.com/product/plants-of-the-fiji-islands/16584/ (accessed on 28 September 2024).
5. Thomson, L.A.J.; Bush, D.; Lesubula, M. Participatory Value Chain Study for Yasi Sandalwood (*Santalum Yasi*) in Fiji. *Australian Forestry* **2020**, *83*, 227–237, doi:10.1080/00049158.2020.1841442.
6. *Santalum Yasi*. *Wikipedia* 2024.
7. Solanki, N.S.; Chauhan, C.S.; Vyas, B.; Marothia, D. Santalum Album Linn: A Review. 12.
8. (PDF) Assessing Genetic Diversity of Natural and Hybrid Populations of Santalum Yasi in Fiji and Tonga Available online: https://www.researchgate.net/publication/299425345_Assessing_genetic_diversity_of_natural_and_hybrid_populations_of_Santalum_yasi_in_Fiji_and_Tonga (accessed on 23 March 2025).
9. ThriftBooks Secrets of Fijian Medicine Book by Michael A Weiner Available online: https://www.thriftbooks.com/w/secrets-of-fijian-medicine_unknown/22012057/ (accessed on 12 July 2025).
10. Struthers, R.; Lamont, B.B.; Fox, J.E.D.; Wijesuriya, S.; Crossland, T. Mineral Nutrition of Sandalwood (*Santalum Spicatum*). *J Exp Bot* **1986**, *37*, 1274–1284, doi:10.1093/jxb/37.9.1274.
11. Ochi, T.; Shibata, H.; Higuti, T.; Kodama, K.; Kusumi, T.; Takaishi, Y. Anti- *Helicobacter p Ylori* Compounds from *Santalum a Lbum*. *Journal of Natural Products* **2005**, *68*, 819–824, doi:10.1021/np040188q.
12. Kuttan, R.; Nair, N.G.; Radhakrishnan, A.N.; Spande, T.F.; Yeh, H.J.; Witkop, B. Isolation and Characterization of γ-L-Glutamyl-S-(Trans-1-Propenyl)-L-Cysteine Sulfoxide from Sandal (Santalum Album). Interesting Occurrence of Sulfoxide Diastereoisomers in Nature. *Biochemistry* **1974**, *13*, 4394–4400, doi:10.1021/bi00718a024.
13. Butaud, J.-F.; Raharivelomanana, P.; Bianchini, J.-P.; Gaydou, E.M. Santalum Insulare Acetylenic Fatty Acid Seed Oils: Comparison within the Santalum Genus. *J Am Oil Chem Soc* **2008**, *85*, 353–356, doi:10.1007/s11746-008-1196-z.
14. Howes, M.-J.R.; Simmonds, M.S.J.; Kite, G.C. Evaluation of the Quality of Sandalwood Essential Oils by Gas Chromatography–Mass Spectrometry. *Journal of Chromatography A* **2004**, *1028*, 307–312, doi:10.1016/j.chroma.2003.11.093.
15. Kupchan, S.M.; Stevens, K.L.; Rohlfing, E.A.; Sickles, B.R.; Sneden, A.T.; Miller, R.W.; Bryan, R.F. Tumor Inhibitors. 126. New Cytotoxic Neolignans from Aniba Megaphylla Mez. *J. Org. Chem.* **1978**, *43*, 586–590, doi:10.1021/jo00398a013.
16. Sephadex | Sigma-Aldrich Available online: https://www.sigmaaldrich.com/GB/en/search/sephadex?focus=products&page=1&perpage=30&sort=relevance&term=sephadex&type=product (accessed on 23 March 2025).
17. Fred W. McLafferty. Interpretation of Mass Spectra, Third Edition. University Science Books, Mill Valley, California, 1980. Pp. Xvii + 303 - White V - 1982 - Biological Mass Spectrometry - Wiley Online Library Available online: http://onlinelibrary.wiley.com/doi/10.1002/bms.1200090610/abstract (accessed on 16 November 2016).
18. Pellegrin, V. Molecular Formulas of Organic Compounds: The Nitrogen Rule and Degree of Unsaturation. *J. Chem. Educ.* **1983**, *60*, 626, doi:10.1021/ed060p626.
19. CASE NMR Software | Structure Elucidator Suite Available online: https://www.acdlabs.com/products/spectrus-platform/structure-elucidator-suite/ (accessed on 15 September 2023).
20. Bremser, W. Hose — a Novel Substructure Code. *Analytica Chimica Acta* **1978**, *103*, 355–365, doi:10.1016/S0003-2670(01)83100-7.
21. Elyashberg, M.; Williams, A. ACD/Structure Elucidator: 20 Years in the History of Development. *Molecules* **2021**, *26*, 6623, doi:10.3390/molecules26216623.
22. Rateb, M.E.; Tabudravu, J.; Ebel, R. NMR Characterisation of Natural Products Derived from Under-Explored Microorganisms. In *Nuclear Magnetic Resonance*; Ramesh, V., Ed.; Royal Society of Chemistry: Cambridge, 2016; Vol. 45, pp. 240–268 ISBN 978-1-78262-053-2.
23. Elyashberg, M.; Williams, A.J.; Blinov, K. Structural Revisions of Natural Products by Computer-Assisted Structure Elucidation (CASE) Systems. *Natural Product Reports* **2010**, *27*, 1296, doi:10.1039/c002332a.

24. ACD/MS FragmenterMass Spectral Fragmentation Analysis Software Cited December 2005 [Http://Www.Acdlabs.Com] Cited December 2005.
25. Elyashberg, M.E.; Williams, A.; Blinov, K. *Contemporary Computer-Assisted Approaches to Molecular Structure Elucidation*; New Developments in NMR; The Royal Society of Chemistry, 2012; ISBN 978-1-84973-432-5.
26. Atropisomer. *Wikipedia* 2025.
27. Smyth, J.E.; Butler, N.M.; Keller, P.A. A Twist of Nature – the Significance of Atropisomers in Biological Systems. *Nat. Prod. Rep.* **2015**, *32*, 1562–1583, doi:10.1039/C4NP00121D.
28. PerkinElmer ChemDraw Professional. Get the Software Safely and Easily. Available online: https://perkinelmer-chemdraw-professional.software.informer.com/16.0/ (accessed on 29 March 2025).
29. Fragkiadakis, M.; Thomaidi, M.; Stergiannakos, T.; Chatziorfanou, E.; Gaidatzi, M.; Michailidis Barakat, A.; Stoumpos, C.; Neochoritis, C.G. High Rotational Barrier Atropisomers. *Chemistry – A European Journal* **2024**, *30*, e202401461, doi:10.1002/chem.202401461.
30. Lanman, B.A.; Parsons, A.T.; Zech, S.G. Addressing Atropisomerism in the Development of Sotorasib, a Covalent Inhibitor of KRAS G12C: Structural, Analytical, and Synthetic Considerations. *Acc. Chem. Res.* **2022**, *55*, 2892–2903, doi:10.1021/acs.accounts.2c00479.
31. Parker, D.; Taylor, R.J.; Ferguson, G.; Tonge, A. Origins of the Proton NMR Chemical Shift Non-Equivalence in the Diastereotopic Methylene Protons of Camphanamides. *Tetrahedron* **1986**, *42*, 617–622, doi:10.1016/S0040-4020(01)87461-5.
32. PubChem Methyl (11E,13E)-Octadeca-11,13-Dien-9-Ynoate Available online: https://pubchem.ncbi.nlm.nih.gov/compound/92040344 (accessed on 20 March 2025).
33. Methyl 9,11-Octadecadiynoate - PubChem Compound - NCBI Available online: https://www.ncbi.nlm.nih.gov/pccompound?cmd=HistorySearch&WebEnvRq=1&hinit=true&WebEnv=MCID_67dc47eec9279463e904ca69&query_key=1 (accessed on 20 March 2025).
34. Askari, A.; Worthen, L.R.; Shimizu, Y. Gaylussacin, a New Stilbene Derivative from Species of Gaylussacia. *Lloydia* **1972**, *35*, 49–54.
35. Chrysin-7beta-Monoglucoside - PubChem Compound - NCBI Available online: https://www.ncbi.nlm.nih.gov/pccompound/?term=chrysin+monoglucoside (accessed on 23 March 2025).
36. Chrysin-7beta-Monoglucoside - Chemical Compound | PlantaeDB Available online: https://plantaedb.com/compounds/chrysin-7beta-monoglucoside (accessed on 23 March 2025).
37. PubChem Neoschaftoside Available online: https://pubchem.ncbi.nlm.nih.gov/compound/442619 (accessed on 23 March 2025).
38. Besson, E.; Chopin, J.; R. Markham, K.; Mues, R.; Wong, H.; Bouillant, M.-L. Identification of Neoschaftoside as 6-C-β-d-Glucopyranosyl-8-C-β-l-Arabinopyranosylapigenin. *Phytochemistry* **1984**, *23*, 159–161, doi:10.1016/0031-9422(84)83098-8.
39. PubChem Chrysin 6-C-Glucoside 8-C-Arabinoside Available online: https://pubchem.ncbi.nlm.nih.gov/compound/21722007 (accessed on 23 March 2025).
40. Lab Equipment and Lab Supplies | Fisher Scientific Available online: https://www.fishersci.co.uk/gb/en/home.html (accessed on 19 June 2023).
41. Stable Isotopes, NMR Solvents and Tubes Available online: https://www.ukisotope.com/ (accessed on 13 June 2025).
42. LC/MS Instruments, HPLC MS, LC/MS Systems, LC/MS Analysis | Agilent Available online: https://www.agilent.com/en/product/liquid-chromatography-mass-spectrometry-lc-ms/lc-ms-instruments/quadrupole-time-of-flight-lc-ms (accessed on 8 August 2023).

43. FTIR Spectroscopy Available online: https://www.shimadzu.com/an/products/molecular-spectroscopy/ftir/index.html (accessed on 13 June 2025).
44. University of Edinburgh – Connect NMR UK Available online: https://www.connectnmruk.ac.uk/facility/edinburgh-university/ (accessed on 26 January 2025).
45. Marine Biodiscovery | The School of Natural and Computing Sciences | The University of Aberdeen Available online: https://www.abdn.ac.uk/ncs/departments/chemistry/research/marine-biodiscovery/ (accessed on 23 March 2025).
46. Agilent MassHunter Software | Agilent Available online: https://www.agilent.com/en/promotions/masshunter-mass-spec (accessed on 11 November 2024).
47. Phenomenex UHPLC, HPLC, SPE, GC - Leader in Analytical Chemistry Solutions Available online: https://www.phenomenex.com/?gclid=EAIaIQobChMIlYLs75LP_wIVw9_tCh0eAgYsEAAYASAAEgJA4PD_BwE (accessed on 19 June 2023).
48. Quadrupole Spectrometer - maXis II™ - Bruker Daltonics - TOF-MS / MS/MS / for Pharmaceutical Applications Available online: https://www.directindustry.com/prod/bruker-daltonics/product-30029-991983.html (accessed on 30 March 2025).
49. Sephadex. *Wikipedia* 2023.
50. Solid Phase Extraction (SPE) Method Development Tool from Phenomenex Available online: https://www.phenomenex.com/Tools/SPEMethodDevelopment (accessed on 10 January 2017).
51. Google Maps Available online: https://www.google.com/maps/place/Koronivia/@-18.0499986,178.5127337,8040m/data=!3m1!1e3!4m14!1m7!3m6!1s0x6e1be1dc6b6b9e01:0x3298dfc740562b9!2sKoronivia!8m2!3d-18.05!4d178.5333333!16s%2Fg%2F11cnyr0crw!3m5!1s0x6e1be1dc6b6b9e01:0x3298dfc740562b9!8m2!3d-18.05!4d178.5333333!16s%2Fg%2F11cnyr0crw?entry=ttu (accessed on 31 October 2023).
52. The Institute of Applied Sciences - The Institute of Applied Sciences Available online: https://www.usp.ac.fj/the-institute-of-applied-sciences/ (accessed on 23 March 2025).
53. South Pacific Regional Herbarium and Biodiversity Centre Available online: https://www.usp.ac.fj/the-institute-of-applied-sciences/south-pacific-regional-herbarium-and-biodiversity-centre/ (accessed on 14 October 2023).
54. Tabudravu, J.N.; Jaspars, M. Stelliferin Riboside, a Triterpene Monosaccharide Isolated from the Fijian Sponge *Geodia g Lobostellifera*. *Journal of Natural Products* **2001**, *64*, 813–815, doi:10.1021/np010019v.
55. Schlüter, L.; Hansen, K.Ø.; Isaksson, J.; Andersen, J.H.; Hansen, E.H.; Kalinowski, J.; Schneider, Y.K.-H. Discovery of Thiazostatin D/E Using UPLC-HR-MS2-Based Metabolomics and σ-Factor Engineering of Actinoplanes Sp. SE50/110. *Front. Bioeng. Biotechnol.* **2024**, *12*, doi:10.3389/fbioe.2024.1497138.
56. Basic Colorimetric Proliferation Assays: MTT, WST, and Resazurin | Springer Nature Experiments Available online: https://experiments.springernature.com/articles/10.1007/978-1-4939-6960-9_1 (accessed on 30 March 2025).
57. Koagne, R.R.; Annang, F.; Cautain, B.; Martín, J.; Pérez-Moreno, G.; Bitchagno, G.T.M.; González-Pacanowska, D.; Vicente, F.; Simo, I.K.; Reyes, F.; et al. Cytotoxycity and Antiplasmodial Activity of Phenolic Derivatives from Albizia Zygia (DC.) J.F. Macbr. (Mimosaceae). *BMC Complement Med Ther* **2020**, *20*, 8, doi:10.1186/s12906-019-2792-1.
58. Audoin, C.; Bonhomme, D.; Ivanisevic, J.; Cruz, M.D. la; Cautain, B.; Monteiro, M.C.; Reyes, F.; Rios, L.; Perez, T.; Thomas, O.P. Balibalosides, an Original Family of Glucosylated Sesterterpenes Produced by the Mediterranean Sponge Oscarella Balibaloi. *Marine Drugs* **2013**, *11*, 1477–1489, doi:10.3390/md11051477.
59. Vickery, J.R.; Whitfield, F.B.; Ford, G.L.; Kennett, B.H. Ximenynic Acid inSantalum Obtusifolium Seed Oil. *J Am Oil Chem Soc* **1984**, *61*, 890–891, doi:10.1007/BF02542158.
60. Cai, F.; Hettiarachchi, D.; Hu, X.; Singh, A.; Liu, Y.; Sunderland, B. Chapter 20 - Ximenynic Acid and Its Bioactivities. In *Advances in Dietary Lipids and Human Health*; Li, D., Ed.; Academic Press, 2022; pp. 303–328 ISBN 978-0-12-823914-8.

61. XYMENYNIC ACID - Cosmetics Ingredient INCI Available online: https://cosmetics.specialchem.com/inci-ingredients/xymenynic-acid (accessed on 25 May 2025).
62. Li, X.-C.; Jacob, M.R.; ElSohly, H.N.; Nagle, D.G.; Smillie, T.J.; Walker, L.A.; Clark, A.M. Acetylenic Acids Inhibiting Azole-Resistant Candida Albicans from Pentagonia Gigantifolia. *J. Nat. Prod.* **2003**, *66*, 1132–1135, doi:10.1021/np030196r.
63. Li, X.-C.; Jacob, M.R.; Khan, S.I.; Ashfaq, M.K.; Babu, K.S.; Agarwal, A.K.; ElSohly, H.N.; Manly, S.P.; Clark, A.M. Potent In Vitro Antifungal Activities of Naturally Occurring Acetylenic Acids. *Antimicrob Agents Chemother* **2008**, *52*, 2442–2448, doi:10.1128/AAC.01297-07.
64. Okada, S.; Zhou, X.-R.; Damcevski, K.; Gibb, N.; Wood, C.; Hamberg, M.; Haritos, V.S. Diversity of Δ12 Fatty Acid Desaturases in Santalaceae and Their Role in Production of Seed Oil Acetylenic Fatty Acids *. *Journal of Biological Chemistry* **2013**, *288*, 32405–32413, doi:10.1074/jbc.M113.511931.
65. Sperling, P.; Lee, M.; Girke, T.; Zähringer, U.; Stymne, S.; Heinz, E. A Bifunctional Δ6-Fatty Acyl Acetylenase/Desaturase from the Moss Ceratodon Purpureus. *European Journal of Biochemistry* **2000**, *267*, 3801–3811, doi:10.1046/j.1432-1327.2000.01418.x.
66. Vierengel, A.; Kohn, G.; Vandekerkhove, O.; Hartmann, E. 9-Octadecen-6-Ynoic Acid from Riccia Fluitans. *Phytochemistry* **1987**, *26*, 2101–2102, doi:10.1016/S0031-9422(00)81767-7.
67. Acetylenic FA | Cyberlipid.
68. Minto, R.E.; Blacklock, B.J. Biosynthesis and Function of Polyacetylenes and Allied Natural Products. *Prog Lipid Res* **2008**, *47*, 233–306, doi:10.1016/j.plipres.2008.02.002.
69. Ondeyka, J.G.; Zink, D.L.; Young, K.; Painter, R.; Kodali, S.; Galgoci, A.; Collado, J.; Tormo, J.R.; Basilio, A.; Vicente, F.; et al. Discovery of Bacterial Fatty Acid Synthase Inhibitors from a Phoma Species as Antimicrobial Agents Using a New Antisense-Based Strategy. *J Nat Prod* **2006**, *69*, 377–380, doi:10.1021/np050416w.
70. Tobinaga, S.; Sharma, M.; Aalbersberg, W.; Watanabe, K.; Iguchi, K.; Narui, K.; Sasatsu, M.; Waki, S. Isolation and Identification of a Potent Antimalarial and Antibacterial Polyacetylene from *Bidens Pilosa*. *Planta Med* **2009**, *75*, 624–628, doi:10.1055/s-0029-1185377.
71. da Silva, J.; Cerdeira, C.D.; Chavasco, J.M.; Cintra, A.B.P.; da Silva, C.B.P.; de Mendonça, A.N.; Ishikawa, T.; Boriollo, M.F.G.; Chavasco, J.K. In Vitro SCREENING ANTIBACTERIAL ACTIVITY OF Bidens Pilosa LINNÉ AND Annona Crassiflora MART. AGAINST OXACILLIN RESISTANT Staphylococcus Aureus (ORSA) FROM THE AERIAL ENVIRONMENT AT THE DENTAL CLINIC. *Rev Inst Med Trop Sao Paulo* **2014**, *56*, 333–340, doi:10.1590/S0036-46652014000400011.
72. Yan, Z.; Chen ,Zhenshan; Zhang ,Ling; Wang ,Xiaoming; Zhang ,Yaowen; and Tian, Z. Bioactive Polyacetylenes from Bidens Pilosa L and Their Anti-Inflammatory Activity. *Natural Product Research* **2022**, *36*, 6353–6358, doi:10.1080/14786419.2022.2029432.
73. Santalaceae. *Wikipedia* 2025.
74. Teka, T.; Zhang, L.; Ge, X.; Li, Y.; Han, L.; Yan, X. Stilbenes: Source Plants, Chemistry, Biosynthesis, Pharmacology, Application and Problems Related to Their Clinical Application-A Comprehensive Review. *Phytochemistry* **2022**, *197*, 113128, doi:10.1016/j.phytochem.2022.113128.
75. Chong, J.; Poutaraud, A.; Hugueney, P. Metabolism and Roles of Stilbenes in Plants. *Plant Science* **2009**, *177*, 143–155, doi:10.1016/j.plantsci.2009.05.012.
76. Ahamad, J.; Ismail, S.A.; Jalal, A.Z.; Akhtar, M.S.; Ahmad, J. Stilbenes in Breast Cancer Treatment: Nanostilbenes an Approach to Improve Therapeutic Efficacy. *Pharmacological Research - Natural Products* **2025**, *6*, 100173, doi:10.1016/j.prenap.2025.100173.

77. Lee, Y.-H.; Chen, Y.-Y.; Yeh, Y.-L.; Wang, Y.-J.; Chen, R.-J. Stilbene Compounds Inhibit Tumor Growth by the Induction of Cellular Senescence and the Inhibition of Telomerase Activity. *International Journal of Molecular Sciences* **2019**, *20*, 2716, doi:10.3390/ijms20112716.

78. Sirerol, J.A.; Rodríguez, M.L.; Mena, S.; Asensi, M.A.; Estrela, J.M.; Ortega, A.L. Role of Natural Stilbenes in the Prevention of Cancer. *Oxidative Medicine and Cellular Longevity* **2016**, *2016*, 3128951, doi:10.1155/2016/3128951.

79. Tian, J.; Jin, L.; Liu, H.; Hua, Z. Stilbenes: A Promising Small Molecule Modulator for Epigenetic Regulation in Human Diseases. *Front Pharmacol* **2023**, *14*, 1326682, doi:10.3389/fphar.2023.1326682.

80. Piekuś-Słomka, N.; Mikstacka, R.; Ronowicz, J.; Sobiak, S. Hybrid Cis-Stilbene Molecules: Novel Anticancer Agents. *Int J Mol Sci* **2019**, *20*, 1300, doi:10.3390/ijms20061300.

81. Breast Cancer Prevention: Tamoxifen and Raloxifene Available online: https://www.cancer.org/cancer/types/breast-cancer/risk-and-prevention/tamoxifen-and-raloxifene-for-breast-cancer-prevention.html (accessed on 24 May 2025).

82. Basilaia, M.; Chen, M.H.; Secka, J.; Gustafson, J.L. Atropisomerism in the Pharmaceutically Relevant Realm. *Acc. Chem. Res.* **2022**, *55*, 2904–2919, doi:10.1021/acs.accounts.2c00500.